

Simulations of the Patterns of the Intermediate State in Type-I Superconductors

Alexander D. Hernández and Daniel Domínguez
*Centro Atómico Bariloche and Instituto Balseiro,
8400 San Carlos de Bariloche, Río Negro, Argentina.*

We present simulations of the intermediate state of type-I superconducting films solving the time dependent Ginzburg-Landau equations, which include the demagnetizing fields via the Biot-Savart law. For small square samples we find that, when slowly increasing the applied magnetic field H_a , there is a saw-tooth behavior of the magnetization and very geometric patterns, due to the influence of surface barriers; while when slowly decreasing H_a , there is a positive magnetization and symmetry-breaking structures. When random initial conditions are considered, we obtain droplet and labyrinthine striped patterns, depending on H_a , as observed in experiments.

PACS numbers: 74.25.-q, 74.25.Ha, 75.60.-d

In 1937 Landau modeled the intermediate state (IS) in thin slabs of type-I superconductors, assuming a periodic structure of alternating stripes of normal and superconducting phases [1]. Direct experimental observation of the IS revealed that, while in some cases its structure resembled the Landau picture, very complex patterns and history dependence were usually seen. [2, 3, 4, 5, 6, 7] Similar type of complex structures were later observed in two-dimensional (2D) systems where there is a competition among interfacial tension and long-range interactions [8] like thin magnetic films [9], ferromagnetic fluids [10], Langmuir and lipid monolayers [11], and self-assembled atoms on solid surfaces [12]. Labyrinthine patterns, and a transition from structures of droplets to stripes are typically observed. [8] The rich physics found in these 2D systems has motivated a renewed interest in the study of the IS in type-I superconductors in several recent experiments. [13, 14, 15, 16, 17, 18] Moreover, it has been shown recently that the core of neutron stars forms a type-I proton superconductor, where the existence of an IS could explain the long precession periods observed in these stars [19].

Little theoretical progress [20, 21, 22, 23, 24, 25] has been made since Landau in the understanding of the non-periodic patterns of the IS. Only recently a current-loop model [26] gives a good description of the structure of the IS, where the long-range magnetic interactions are considered in detail. However, the interface energy is treated approximately and no deduction of the model from the more general Ginzburg-Landau free energy is given [27].

In this letter we perform detailed and realistic simulations of a type-I superconductor by solving the time dependent Ginzburg-Landau (TDGL) equations for a superconducting slab of thickness d . We consider the “non-branching case”, where $d \ll d_s \approx 800(\xi - \lambda)$ [21], which can be well approximated by reducing the equations to a 2D problem, as done for example in Ref [20, 26]. We therefore assume that the current density \mathbf{J} and the order parameter Ψ can be replaced by their average over z for $-d/2 < z < d/2$, i.e. $\mathbf{J}(\mathbf{R}, z) \rightarrow \mathbf{J}(\mathbf{R})$ and

$\Psi(\mathbf{R}, z) \rightarrow \Psi(\mathbf{R})$, with $\mathbf{R} = (x, y)$ the in-plane coordinate. The TDGL equations [25, 26] are, in the gauge where the electrostatic potential is zero,

$$\frac{\partial \Psi}{\partial t} = \frac{1}{\tau_G} (|\Psi|^2 - 1) \Psi - \frac{\xi^2}{\tau_G} \left(\nabla - i \frac{2e}{\hbar c} \mathbf{A} \right)^2 \Psi \quad (1)$$

$$\mathbf{J} = \frac{1}{8\pi e \lambda^2} \text{Im} \left[\Psi^* \left(\nabla - i \frac{2e}{\hbar c} \mathbf{A} \right) \Psi \right] - \frac{\sigma_n}{c} \frac{\partial \mathbf{A}}{\partial t} \quad (2)$$

Here ∇ , \mathbf{A} , \mathbf{J} are 2D in-plane vectors, $\tau_G = \xi^2/D$, D is the diffusion constant, σ_n the normal state conductivity, $\lambda(T)$ the penetration depth and $\xi(T)$ the coherence length. These 2D approximated TDGL equations couple with the perpendicular component of \mathbf{B} . Following Ref.[28] we express the z -averaged sheet current \mathbf{J} by a scalar function g : $\mathbf{J}(\mathbf{R}) = \nabla \times \hat{\mathbf{z}}g(\mathbf{R})$. This guarantees that $\nabla \cdot \mathbf{J} = 0$, the physical meaning of $g(\mathbf{R})$ being the local magnetization or density of tiny current loops. Next one relates $g(\mathbf{R})$ with $B_z(\mathbf{r}) = \nabla \times \mathbf{A}|_z$ at $z = 0$ and the applied field H_a by means of the Biot-Savart law [28]:

$$B_z(\mathbf{R}, z = 0) = H_a + \frac{1}{c} \int Q(\mathbf{R}, \mathbf{R}') g(\mathbf{R}') d^2 \mathbf{R}' \quad (3)$$

The kernel Q satisfies $Q(\mathbf{R}_1, \mathbf{R}_2) \equiv Q(\mathbf{R}_2 - \mathbf{R}_1)$; $Q(R \gg d) = -d/R^3$; and $\int d^2 \mathbf{R} Q(\mathbf{R}) = 0$ (due to flux conservation). To a good approximation the kernel can be given by (see K. Maki in [20]): $Q(\mathbf{R}) = 4\pi\delta(\mathbf{R}) - d/[\|\mathbf{R}\|^2 + d^2/4]^{3/2}$. The boundary conditions are $(\nabla - i \frac{2e}{\hbar c} \mathbf{A})|_{\perp} \Psi = 0$ and $g|_b = 0$.

We solve the equations with a finite difference scheme with discretization $\Delta x = \Delta y = 0.5\xi(0)$, using link variables to maintain the gauge invariance as in [25]. We normalize time by $t_0 = 4\pi\sigma_n\lambda^2/c^2$, \mathbf{A} by $H_{c2}(0)\xi(0)$, T (temperature) by T_c , and take $\tau_G/t_0 = 12$. To obtain $g(\mathbf{R})$ we invert (3) using the conjugate gradient method as done in [29]. We consider thickness $d = 40\xi(0)$; $\kappa = \lambda/\xi = 0.6$; $T = 0.8T_c$ and time step $\Delta t = 0.25$. Square samples of size $L \times L$ with $L = 256\xi(0)$ are studied. We have performed simulations of the intermediate state following three different procedures: (i) slowly increasing the magnetic field from $H_a = 0$, (ii)

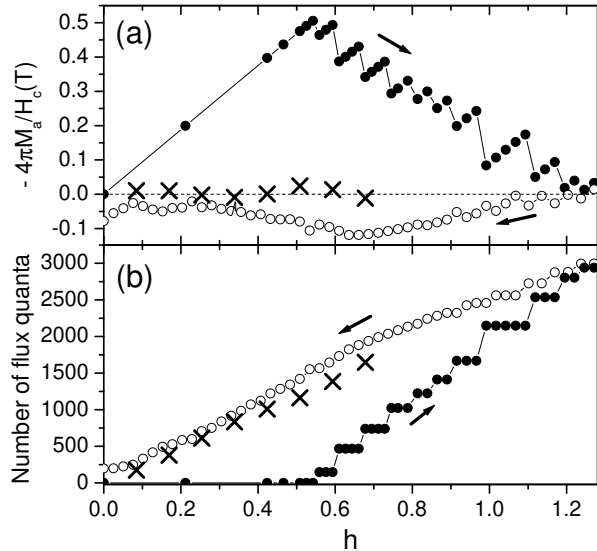


FIG. 1: (a) $-(B - H_a)/H_c(T)$ and (b) the number of flux quanta obtained increasing (closed circles), decreasing (open circles) the external magnetic field $h = H_a/H_c(T)$, and with random initial conditions (crosses).

slowly decreasing the magnetic field from the normal state ($H_a > H_c$) and (iii) starting from random initial conditions for each value of H_a . The global results for the three cases are summarized in Figure 1. We show the apparent magnetization, $4\pi M_a = \langle B_z \rangle - H_a$ (real magnetization is $4\pi M = B - H$, but M_a is what can be determined experimentally), in Fig.1(a), and the number of flux quanta inside the sample, $N\Phi_o = \oint(A + \frac{J_s}{|\Psi|^2})dl$, in Fig.1(b), as a function of $h = H_a/H_c(T)$.

(i) *Slowly increasing the magnetic field.* We start from $H_a = 0$ with a state with $|\Psi|^2 = 1$ and $B = 0$ and increase H_a in small steps, after reaching a stationary state for each field (when $|\Delta E/E| < 10^{-6}$; where ΔE is the change in energy between consecutive time steps). We observe a Meissner state for $H_a < H_p = 0.56H_c$. Surface barriers preclude the penetration of flux below H_p . It is known that the surface barrier in macroscopic type-I superconductors leads to large first penetration fields H_p , which depend on the sample shape and dimensions [13, 23]. Here the smallness of our system enhances this effect. We observe that at $H \gtrsim H_p$ four long chunks of the normal phase, carrying hundreds of flux quanta, enter from each side of the square and equilibrate in the pattern shown in Fig.2(a). At a higher field $H_{p,2}$, some other four chunks of flux enter and form the pattern seen in Fig.2(b). Further increasing the field, more complex structures form, as shown in Fig.2(c) and (d). Above H_c , flux has fully entered inside the sample and there is only surface superconductivity until $H_{c3} > H_c$. All the patterns of the IS observed follow the geometry of the sample and have the symmetry of the square. In general,

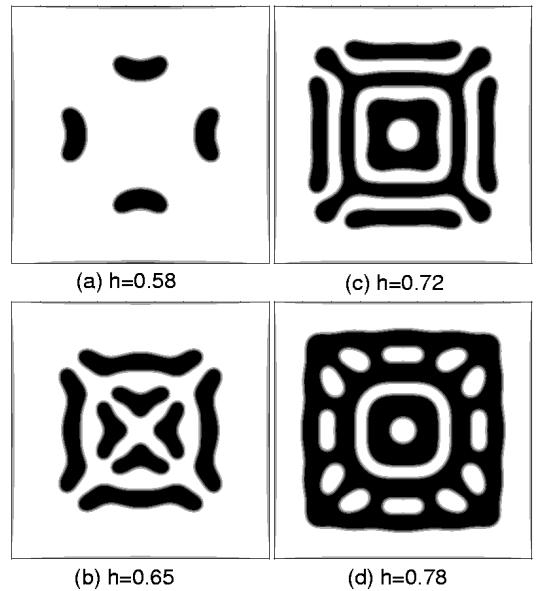


FIG. 2: Spatial patterns of the magnitude of the order parameter $|\Psi(r)|^2$ obtained continuously increasing $h = H_a/H_c$ from $h = 0$. Gray scale ranging from black for $|\Psi(r)|^2 = 0$ to white for $|\Psi(r)|^2 = 1$. For $\kappa = 0.6$, $d = 40\xi(0)$ and sample size $256\xi(0) \times 256\xi(0)$.

we find that the entrance of the normal phase occurs only for discrete values of penetration fields $H_{p,i}$ where several flux quanta are nucleated at the four sides of the square, while for $H_{p,i} < H_a < H_{p,i+1}$, there is no flux entrance. This shows up as a series of plateaus and jumps in the number of flux quanta vs. H_a in Fig.1(b) and as a sawtooth behavior in the magnetization in Fig.1(a). This type of behavior reminds us of the results observed in mesoscopic type-II systems [30] which also show a sawtooth behavior of the magnetization. The main difference is that while in [30] each jump in M_a corresponds to the entrance of one quantum of flux (one vortex), here at each jump in M_a several hundreds of flux quanta have entered. In both cases, the predominant feature is the dominance of surface barriers and geometry effects due to the smallness of the sample.

(ii) *Slowly decreasing the magnetic field.* We start from $H_a > H_c$ with a state with $\Psi = 0$ and $B = H_a$ and decrease H_a in small steps, after reaching a stationary state for each field. The resulting intermediate state patterns are shown in Fig.3. When $H_a \approx H_c$ the superconducting phase enters into the sample and the total number of flux quanta is reduced. At first, the superconducting phase forms four chunks embedded within the normal phase, which nearly follow the square symmetry of the system, as shown in Fig.3(a). However, we observe that when decreasing the field the square symmetry is always broken in the patterns. The breaking of symmetry is stronger the further we decrease the field. In this way, labyrinthine

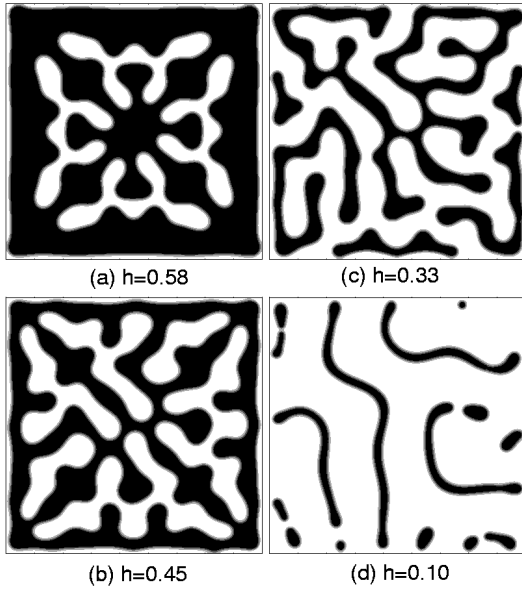


FIG. 3: Spatial patterns of $|\Psi(r)|^2$ obtained decreasing h from the normal state at $h \gg 1$. Same parameters as in Fig.2.

patterns are formed at mid-range fields, as can be seen in Figs.3(b) and (c). In general, the expulsion of flux occurs gradually when decreasing H_a as shown in Fig.1(b). For low fields we see that thin stripes of normal phase are trapped within the sample, as shown in Fig.3(d). The difficulty for expelling flux is due to the surface barrier and results in a positive magnetization as a function of h as shown in Fig.1(a). Even at $h = 0$, a few small thin stripes of flux remain trapped in the sample, as evidenced in Fig.1(b), where the number of flux quanta is finite at $h = 0$, and in Fig.1(a), where $M_a > 0$ at $h = 0$. This agrees with the experiments reported in [4] where it has been observed that some trapped flux remains in the system at $h = 0$ when decreasing the field. Also in [7] a positive magnetization has been obtained when decreasing H_a in Sn films. It is interesting to mention that a similar positive magnetization was observed in mesoscopic type-II superconductors [30] when decreasing H_a , and attributed to the importance of surface barriers.

In the patterns of Fig.3, for slowly decreasing field, there are elongated normal domains with their edges ending near the surface, while in the patterns of Fig.2, for slowly increasing field, the normal domains tend to be in the center of the sample, forming closed structures. Similar differences in the IS have been observed in [2, 3, 4].

(iii) *Random initial conditions.* The structures of the IS discussed above, obtained either increasing or decreasing the magnetic field, are strongly influenced by the surface barriers and/or the geometry of the small sample we can simulate. In a film of large linear size L the demagnetization factor is $\propto 1 - d/L \approx 1$, and therefore we expect that $B \approx H_a$. To obtain stationary states more typical

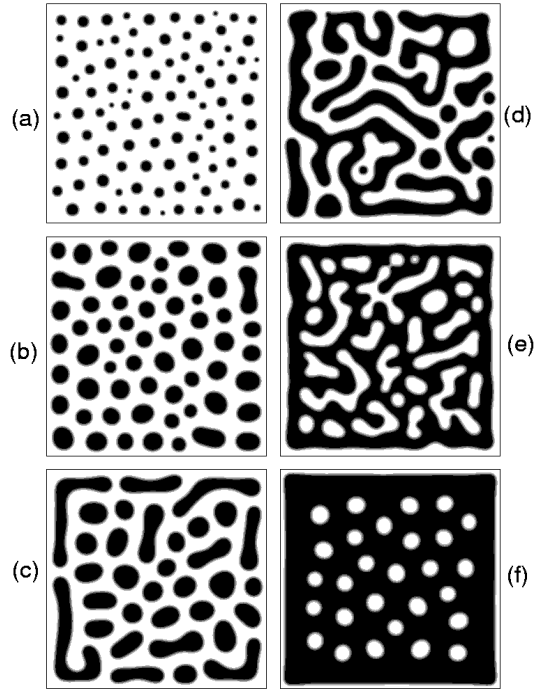


FIG. 4: $|\Psi(r)|^2$ patterns obtained using random initial conditions for (a) $h = 0.17$, (b) $h = 0.33$, (c) $h = 0.42$, (d) $h = 0.50$, (e) $h = 0.58$ and (f) $h = 0.75$. Same parameters as in Fig.2.

of the bulk behavior of large samples, we start with a initial condition with random values of \mathbf{A} and Ψ , such that we satisfy $\langle B \rangle = H_a$ from the start, and that the initial state is superconducting in average, $\langle |\Psi|^2 \rangle > 0$. We performed simulations with this initial condition for different values of h , and let the system to evolve for each case, using a stronger criterion for assuming stationarity: $|\Delta E/E| < 10^{-9}$. We obtain that in the stationary state most of the flux remains inside the sample and $\langle B_z \rangle - H_a \approx 0$ as can be seen in Fig.1(a). The structures obtained are shown in Fig. 4. For low fields, we observe in Fig.4(a) and (b) that the intermediate state consists on almost circular droplets of the normal phase. For higher fields, the droplets start to coalesce into long lamellar-like domains, as seen in Fig.4(c). At intermediate fields, as shown in Figs.4(d) and (e), labyrinthine patterns of stripes of the normal phase are formed. For high fields close to H_c we observe almost circular droplets of the superconducting phase embedded within the mostly normal phase, see Fig.4(f). Similar type of structures, with droplets of one or the other phase at low and high fields, and with labyrinthine patterns of stripes at mid range fields has been observed for example in Figs.2.8(a)-(f) of Ref.[2] for a lead thin film. Also similar types of structures have been reported in Ref.[3, 4, 5, 6, 16].

We analyze the structures obtained in Fig.4, by calculating the spectral transform of the superconducting order parameter, $I(\mathbf{k}) = \left| \int d\mathbf{r} |\Psi(\mathbf{r})|^2 \exp(i\mathbf{k} \cdot \mathbf{r}) \right|^2$, which

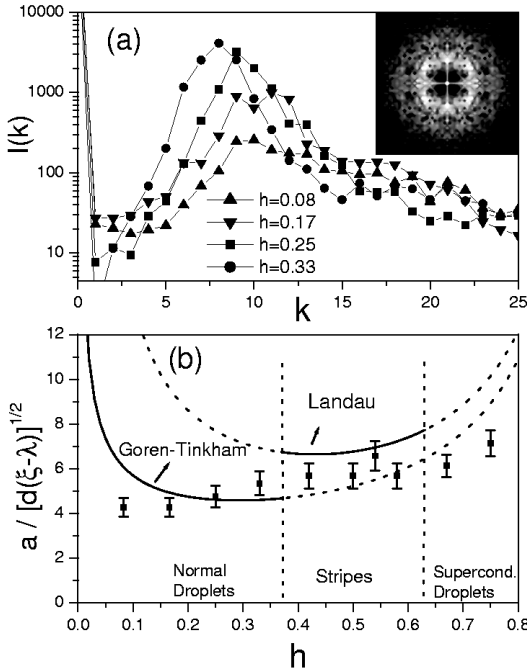


FIG. 5: (a) Spectral intensities obtained from $|\Psi(r)|^2$ at different magnetic fields, a maximum at k_0 is observed. The inset shows the Fourier transform of Fig. 4(a). (b) Periodicity $a = 2\pi/k_0$ of each structure as a function of h . The lines correspond to the Landau and the Goren-Tinkham models.

is shown in Fig.5(a). The non-periodicity and complex structure of the patterns results in very broad maxima in $I(\mathbf{k})$ at finite wave vectors $k_0 = 2\pi/a$ which define a typical length scale a . In the case of low and large fields, a would correspond to the typical distance between droplets, while for mid-range fields, a would correspond to the average widths of the stripes in the labyrinthine patterns. We plot a in Fig.5(b) and compare it with the Landau model of stripes [1] and with a model of Goren and Tinkham for a periodic array of droplets or “flux spots” [22]. We see that the Landau model agrees qualitatively with the results obtained at mid-range h (for these fields the patterns of Fig.4 can have a mixture of “stripes” with a few droplets, which make a smaller than the Landau value). On the other hand, at low h the Goren-Tinkham model does not agree well with the size of the droplets obtained. Also in the experiments of [6] and more recently in [16] it has been found a departure from the Goren-Tinkham model at low fields, while several experiments [3, 5, 6, 14, 16] have found good agreement with the Landau model in the striped patterns.

To summarize, we have been able to reproduce several features of the intermediate state observed in experiments with realistic simulations. Particularly, droplet and labyrinthine striped patterns are obtained depending on the applied field and magnetic history. It will be interesting if experiments on small mesoscopic samples of

type-I superconductors could be performed. Our simulations predict that the strong influence of the surface barriers in small samples will lead to a saw-tooth behavior of the magnetization and very geometric patterns when slowly increasing H_a , and to a positive magnetization and symmetry-breaking structures when slowly decreasing H_a . In conclusion, as a general feature we find that there is an important influence of the initial conditions and magnetic history in the structures of the IS patterns observed, suggesting a complex energy landscape with several competing free energy minima.

We acknowledge discussions with E. Jagla, M. Menghini, F. de la Cruz and financial support from ANPCYT, CNEA and Conicet. ADH acknowledges support from CLAF and Fundación Antorchas.

- [1] L.D. Landau, *Zh. Eskp. Teor. Fiz.* **7**, 371 (1937).
- [2] R.P. Huebener, *Magnetic Flux Structures in Superconductors* (Springer-Verlag, New York, 1979).
- [3] F. Haensler and L. Rinderer, *Helv. Phys. Acta* **40**, 659 (1967).
- [4] R.P. Huebener *et al.* *Cryogenics* **12**, 100 (1972).
- [5] D. E. Farrell *et al.*, *J. Low Temp. Phys.*, **19**, 99 (1975).
- [6] A. Kiendl and H. Kirchner, *J. Low Temp. Phys.*, **14**, 349 (1974).
- [7] R. E. Miller and G. D. Cody, *Phys. Rev.* **173**, 494 (1968).
- [8] M. Seul and D. Andelman, *Science* **267**, 476 (1995).
- [9] M. Seul *et al.*, *Science* **254**, 1616 (1991).
- [10] F. Elias *et al.* *J. Phys. I France* **7**, 711 (1997).
- [11] M. Seul and V. S. Chen, *Phys. Rev. Lett.* **70**, 1658 (1993).
- [12] R. Plass *et al.*, *Nature* **412**, 875 (2001).
- [13] H. Castro *et al.*, *Phys. Rev. B* **59**, 596 (1999).
- [14] C. R. Reisin and S. G. Lipson, *Phys. Rev. B* **61**, 4251 (2000).
- [15] V. S. Egorov *et al.*, *Phys. Rev. B* **64**, 024524 (2001).
- [16] V. Jeudy *et al.*, *Phys. Rev. Lett.* **92**, 147001 (2004).
- [17] R. Prozorov *et al.*, *cond-mat/0409553*.
- [18] M. Menghini *et al.*, unpublished.
- [19] B. Link, *Phys. Rev. Lett.* **91**, 101101 (2003); K. B. Buckley, *ibid.* **92**, 151102 (2004).
- [20] K. Maki, *Ann. Phys.* **34**, 363 (1965); G. Lasher, *Phys. Rev.* **154**, 345 (1967); D.J.E. Callaway, *Ann. Phys.* **213**, 166 (1992).
- [21] A. Hubert, *Phys. Stat. Sol.* **24**, 669 (1967).
- [22] R.N. Goren and M. Tinkham, *J. Low Temp. Phys.* **5**, 465 (1971).
- [23] E. Fortini and E. Paumier, *Phys. Rev. B* **14**, 55 (1976).
- [24] J. M. Simonin and A. López, *J. Low Temp. Phys.* **41**, 105 (1980).
- [25] H. Frahm *et al.*, *Phys. Rev. Lett.* **66**, 3067 (1991); F. Liu *et al.*, *ibid.* **66**, 3071 (1991).
- [26] R.E. Goldstein *et al.*, *Phys. Rev. Lett.* **76**, 3818 (1996); A.T. Dorsey and R.E. Goldstein, *Phys. Rev. B* **57**, 3058 (1998).
- [27] H. Bokil and O. Narayan, *Phys. Rev. B* **56**, 11195 (1997); O. Narayan, *Phys. Rev. Lett.* **81**, 5035 (1998); R. E. Goldstein and A. T. Dorsey, *ibid.* **81**, 5036 (1998).
- [28] E. H. Brandt, *Phys. Rev. Lett.* **74**, 3025 (1995).

[29] D. Domínguez and J.V. José, Phys. Rev. B **53**, 11692 (1996). [30] A. K. Geim *et al.*, Nature **390**, 259 (1997).